
Separable Layers Enable Structured Efficient Linear Substitutions

Gavin Gray, Elliot J. Crowley, Amos Storkey

School of Informatics
University of Edinburgh

{g.d.b.gray, elliot.j.crowley, a.storkey}@ed.ac.uk

Abstract

In response to the development of recent efficient dense layers, this paper shows that something as simple as replacing linear components in pointwise convolutions with structured linear decompositions also produces substantial gains in the efficiency/accuracy tradeoff. Pointwise convolutions are fully connected layers and are thus prepared for replacement by structured transforms. Networks using such layers are able to learn the same tasks as those using standard convolutions, and provide Pareto-optimal benefits in efficiency/accuracy, both in terms of computation (mult-adds) and parameter count (and hence memory). Code is available at <https://github.com/BayesWatch/deficient-efficient>.

1 Introduction

There is continued and pressing need for efficient implementations of neural networks, for example, in real-time processing, and for deployment on embedded devices. Efficiency may be achieved, for example, by inducing sparsity in the trained network (LeCun et al., 1989) or quantisation of the weights being used (Courbariaux et al., 2015). Significant redundancy in the trained parameters used in neural networks allows this (Alvarez & Salzmann, 2016).

A number of methods have reduced stored size or computational cost in neural networks by providing efficient alternatives to fully connected layers; these include HashedNet (Chen et al., 2015), TensorTrain (Novikov et al., 2015) and ACDC (Moczulski et al., 2016). However, as modern neural networks largely avoid fully connected layers, these are not typically considered in a convolutional network setting. Yet, the pointwise convolution in current depthwise-separable layers is a full matrix multiply. In this paper we ask whether methods developed for making fully connected layers efficient provide an effective approach for improving efficiency of convolutional neural networks.

A pointwise convolution is a 1×1 convolution applied at every spatial point on the input tensor; equivalent to a dense layer treating each point as an independent example. Pointwise convolutions consume the vast majority of the parameter and computation budget in competitive image classification architectures (Huang et al., 2017; Zoph & Le, 2017; Liu et al., 2019). In this paper we assess the benefit of substituting a number of structured efficient alternatives in place of these layers and compare the efficiency/accuracy tradeoff on standard benchmark image classification problems.

The main contributions of this paper are:

- A comparison of a number of approaches for replacing dense layers that occur within convolutional blocks (e.g. pointwise layers in separable convolutions), in terms of their efficiency.
- A principled method to tune weight decay when using compressed layers that maintains stability, making substitution more practical.

- Demonstration that the use of these methods provides Pareto-optimal networks, as demonstrated on CIFAR-10, along with characterisation of the compression rates on ImageNet.
- An indication of the best performing and most stable alternative layer parameterisations, to direct practitioners and researchers towards the best network choices.

2 Related Work

Approaches for structured efficient linear layers (SELLs), such as ACDC (Moczulski et al., 2016), differ from other work in efficiency in that they provide a *substitute* to a fully connected layer, but are trained using the same methods that would otherwise be used (e.g. stochastic gradient descent). Other approaches (e.g. Alvarez & Salzmann, 2017) provide an alternative training algorithm for such layers.

In this paper we compare candidate substitute layers; empirically we provide evidence of state-of-the-art performance of some of these approaches on modern fully convolutional networks, which are substantially different from the setting in which many of these methods were proposed. For example, work on SELLs focused on the replacement of fully connected layers in AlexNet (Moczulski et al., 2016; Yang et al., 2015), which now has little relevance to modern convolutional architectures. The ACDC layer (Moczulski et al., 2016) was inspired by circulant transforms and subsequent work has focused on the potential of these transforms (Zhao et al., 2019). Circulant transforms and SELLs were later unified under low displacement rank (LDR) transformations (Zhao et al., 2017; De Sa et al., 2018). Also, circulant transforms have been defined as a special case of unitary group convolution (UGConv) layers (Zhao et al., 2019), allowing a relation to be drawn to the successful ShuffleNet architecture (Zhang et al., 2018).

To summarise, we present strong empirical results on contemporary image classification problems for members of a number of classes of transformations:

- Low-rank substitutions (Alvarez & Salzmann, 2016; Alvarez & Salzmann, 2017; Sainath et al., 2013; Jaderberg et al., 2014; Novikov et al., 2015; Kossaifi et al., 2017; Kim et al., 2015).
- SELLs (Yang et al., 2015; Moczulski et al., 2016; Bojarski et al., 2016).
- Circulant and Block-Circulant layers (Liao et al., 2019; Zhao et al., 2019; Cheng et al., 2015; Araujo et al., 2019).
- Toeplitz-like transforms (Lu et al., 2016; Sindhvani et al., 2015).
- ShuffleNet-like layers (Zhang et al., 2018; Gao et al., 2018).
- Generalised LDR methods (Thomas et al., 2018; De Sa et al., 2018).
- Weight hashing schemes (Chen et al., 2015).

3 Methods

All of the compressed convolutions in this paper are linear reparameterisations of standard convolutions; we demonstrate that when we replace the convolutional layers of modern networks with these compressed reparameterisations, we can achieve high performance for reduced parameter counts and computational cost.

The various substitutions considered are described in Section 3.1. Each either uses fewer parameters, fewer mult-adds or both. These are by no means exhaustive, and have been selected to cover many of the different transformation classes listed in Section 2.

To make training these layers practical, we have to account for the effect of substituting a compressed convolution on the choice for weight decay. We derive the weight decay parameters needed to stabilise training in Section 3.2.

3.1 Substitute Efficient Linear Transforms

Here, we describe each of the methods being compared. All provide an approximation to the operation of a dense random matrix in a linear layer: a matrix-vector product of that matrix with an input vector

of the form $\mathbf{y} = \mathbf{W}\mathbf{x}$, where \mathbf{y} is the output vector, \mathbf{W} is the dense random matrix, and \mathbf{x} is the input vector.

3.1.1 ACDC

In Moczulski et al. (2016), \mathbf{W} is decomposed into a stack of L ACDC layers:

$$\mathbf{W} = \prod_{l=1}^L \mathbf{A}_l \mathbf{C} \mathbf{D}_l \mathbf{C}^{-1} \mathbf{P} \quad (1)$$

where \mathbf{A} and \mathbf{D} are diagonal matrices, \mathbf{C} and \mathbf{C}^{-1} are forward and inverse discrete cosine transforms, and \mathbf{P} is a random permutation matrix. As the operation of a random permutation may be time consuming, we replace \mathbf{P} with a *riffle shuffle*. A riffle shuffle is a fixed permutation, splitting the input in half and then interleaving the two halves (Gilbert, 1955). This was found to work as well as a fixed random permutation and can be evaluated much faster as observed by Zhang et al. (2018). For $\mathbf{W} \in \mathbb{R}^{N \times N}$ the computational complexity is $O(N \log N)$ and storage cost is $O(N)$ (Moczulski et al., 2016).

3.1.2 Tensor-Train

First, we assume it is possible to map a higher dimensional tensor to our weight matrix using a reshape operation: $\mathbf{y} = \mathbf{W}\mathbf{x} = \text{reshape}_{\mathbb{R}^{N \times N}}(\mathcal{A})\mathbf{x}$. This allows us to use a tensor decomposition to represent \mathcal{A} and implement the linear transform using fewer parameters. In Tensor-Train (TT) (Oseledets, 2011), \mathcal{A} is decomposed as:

$$\mathcal{A}(i_1, \dots, i_d) = \mathbf{G}_1(i_1) \dots \mathbf{G}_d(i_d) \quad (2)$$

Where $\mathbf{G}_k(i_k)$ are $r_{k-1} \times r_k$ matrices, with the boundary conditions that ensure $r_0 = r_d = 1$. Each element of the tensor can then be reproduced by performing this sequence of matrix products.

The parameter savings using this method depend on the number of dimensions possessed by the tensor storing the weights. It is possible to perform a matrix-vector, or matrix-matrix, product between two TT tensors. Alternatively, as in our experiments, we can compute the weight matrix from the \mathbf{G}_k factors and backpropagate the error to update those factors with automatic differentiation.

In our experiments we found it best to reshape weight matrices to 3 dimensions, with approximately equal sizes. We then set the TT-rank r_1, \dots, r_{d-1} to control the level of compression. This is in line with previous work substituting TT tensors into fully connected layers of deep neural networks (Novikov et al., 2015).

3.1.3 Tucker decomposition

The Tucker decomposition also decomposes a tensor $\mathcal{A} \in \mathbb{R}^{I_0, \dots, I_d}$, but in this case uses a low rank core $\mathcal{G} \in \mathbb{R}^{R_0, \dots, R_d}$ projected by factors $\mathbf{U}_k \in \mathbb{R}^{R_k, I_k}$ (Kim et al., 2015):

$$\mathcal{A} = \mathcal{G} \times_0 \mathbf{U}_0 \dots \times_d \mathbf{U}_d \quad (3)$$

Where \times_k denotes the *k-mode product*: a matrix product on dimension k while casting over the remaining dimensions. In our experiments, to compare with TT, we only use the Tucker decomposition to store our weight matrices. As with the TT decomposition, we compute the weight matrix, then backpropagate gradients in order to update the \mathbf{U}_k factors.

3.1.4 Rank-factorised (RF) decomposition

A rank factorised matrix is a linear bottleneck. It is chosen as a baseline against which to compare methods from the literature. In place of a dense matrix we first map an input to a smaller number of dimensions, and then back to the output number of dimensions. This uses two weight matrices

$\mathbf{W}_1 \in \mathbb{R}^{d_{\text{bn}} \times d_{\text{in}}}$ and $\mathbf{W}_2 \in \mathbb{R}^{d_{\text{out}} \times d_{\text{bn}}}$, where the input dimensionality is d_{in} , bottleneck is d_{bn} and output is d_{out} . The linear transformation from an input \mathbf{X} to an output \mathbf{Y} can then be expressed as $\mathbf{y} = \mathbf{W}\mathbf{x} = \mathbf{W}_2\mathbf{W}_1\mathbf{x}$.

This parameterisation can be implemented in popular deep learning frameworks with two linear layers in sequence, and can give significant efficiency benefits. For $d_{\text{in}} = d_{\text{out}} = d$, the number of parameters used by applying a dense weight matrix \mathbf{W} to an input vector is d^2 , while the total parameters used in \mathbf{W}_1 and \mathbf{W}_2 is $\frac{2d^2}{b}$ where $b = \frac{d}{d_{\text{bn}}}$.

3.1.5 HashedNet

A virtual weight matrix \mathbf{V} is built from real weights \mathbf{w} using a hash function \mathbf{h} to index those weights:

$$y_i = \sum_{j=1}^N V_{ij}x_j = \sum_{j=1}^N w_{h(i,j)}x_j \quad (4)$$

HashedNets use a hash function to retrieve the weights used in their network (Chen et al., 2015). The particular hash function used in this case takes as input indices in the *virtual* weight matrix, \mathbf{V} , used in the linear transformation, and produces as output a single index into a set of *real* weights \mathbf{w} . As the compression only depends on the number of virtual weights we choose to use, this method is extremely flexible for storage compression. Note that some virtual weights may not be used, as described in Appendix A.

3.1.6 Linearised ShuffleNet

The Shufflenet unit (Zhang et al., 2018) can be related to circulant transforms like ACDC (Moczulski et al., 2016) by defining a generalised UGConv block (Zhao et al., 2019). Unlike applications of circulant transforms, these units are used to implement a state-of-the-art image classification architecture (ShuffleNet). We propose a linear version of the unit, represented by:

$$\mathbf{y} = \mathbf{W}\mathbf{x} = \mathbf{B}_2\mathbf{P}\mathbf{B}_1\mathbf{x} \quad (5)$$

where \mathbf{B}_1 and \mathbf{B}_2 are block diagonal matrices implemented by grouped 1×1 convolutions, and \mathbf{P} is a permutation implemented by a riffle shuffle. While this was not proposed in the literature as a method to compress a linear transformation, the building blocks involved are similar to those used in the ACDC structured efficient linear transformation and so we consider it here.

3.2 Compression Ratio Scaled Weight Decay

One way to motivate L2 regularisation in neural networks is to say that it is equivalent to MAP inference with a Gaussian prior on the weights (Murphy, 2012, p.225). In the context of changing layer structure, we would wish to preserve the total variance of the weight matrix prior under the layer replacement. As the number of parameters tends towards the number in the full weight matrix, we will then tend toward the original weight decay factor. Under the simplifying assumption that the weights, $\{w_n\}_{n=1}^N$ are Gaussian distributed with variance $\frac{1}{\sqrt{d}}$, where d is the weight decay factor, then total variance is:

$$\sum_{n=1}^N E[w_n^2] = \sum_{n=1}^N \frac{1}{d} E[z^2], \quad (6)$$

where z is Gaussian distributed with variance 1. Then we have:

$$\sum_{n=1}^N \text{Var}(w_n) = \frac{N}{d}. \quad (7)$$

Hence, to maintain total variance for M parameters in the compressed layer, we must use the scaled weight decay term:

$$d_c = \frac{Md}{N}. \quad (8)$$

In practice this means multiplying the weight decay factor for compressed weight matrices by the compression ratio M/N . In Figure 6, it is illustrated that this stabilises training and improves performance. It has the desirable property of providing a smooth interpolation to an uncompressed matrix – where the weight decay would be the default. We refer to this approach as *compression ratio scaled* (CRS) weight decay.

4 Experiments

We train networks where each pointwise (1×1) convolution in a base network is substituted for a particular linear transform from Section 3.1. To recapitulate, these transforms are: ACDC, Tensor-Train, Tucker decomposition, Rank-factorised (RF) decomposition, HashedNet, and Linearised ShuffleNet. Each of these substitutions has a tuning parameter that can be altered to determine the number of parameters utilised, allowing us to compare networks for a range of parameter budgets. We perform experiments on CIFAR-10 (Krizhevsky, 2009) with (i) Wide-ResNets (WRN) (Zagoruyko & Komodakis, 2016), specifically WRN-28-10, and (ii) the network discovered by differentiable architecture search (DARTS) (Liu et al., 2019) as base networks. We also experiment on ImageNet (Russakovsky et al., 2015) with WRN-50-2 as a base network. We chose parameter budgets over which networks with each substitution under consideration would have support (see Appendix B). When training:

1. We perform *attention transfer* (AT) (Zagoruyko & Komodakis, 2017) on each substitute network with a trained version of the original base network as a teacher.
2. We utilise *CRS weight decay*, as defined in Section 3.2.

We examine the importance of these choices in Section 5. Our experimental set up is described in detail in Appendix C.

4.1 WRN-28-10 on CIFAR-10

The base WRN-28-10 achieves a top-1 validation error of 3.2% and has 36.5M parameters. We produce substitute networks at three approximate parameter budgets: 2.4M, 1.2M, and 0.6M. Note that these correspond to very high compression rates.

The relationship between the number of parameters used by our substitute WRN-28-10 networks and the top-1 error—through AT with the base network—is illustrated in Figure 1. We report mult-adds where possible in Figure 2.

One might expect HashedNet or Tensor-Train to work best as compression methods, as they do not necessarily reduce the number of mult-adds used by the network. HashedNet, in particular, substitutes a weight matrix of precisely the same size at test time, and applying that weight matrix uses the same number of mult-adds used by the original network. While all of the considered methods produce a network that contains less than 10% the parameters used by the base network while losing only 1% error, HashedNet and Tensor-Train substitutions can maintain this error using *less than 3% of the parameters*. Unfortunately, ACDC was only able to place a single point at the lowest compression ratio. It performs comparably well, but becomes unstable with larger numbers of ACDC layers.

4.2 DARTS net on CIFAR-10

DARTS net is a state-of-the-art image classification network (Liu et al., 2019) achieving 2.83% while using only 3.8M parameters. We use this as a base network, and substitute linear transformations for parameter budgets of 1.42M, 0.83M, and 0.49M. As before, these substitute networks are trained using AT with the base network and CRS weight decay.

The validation errors of these substitute networks against their parameter total is shown in Figure 3. Remarkably, we can achieve compression to 20% of the original number of parameters for HashedNet, ShuffleNet and Tensor-Train substitutions while still being *within 1% the original top-1 error*.

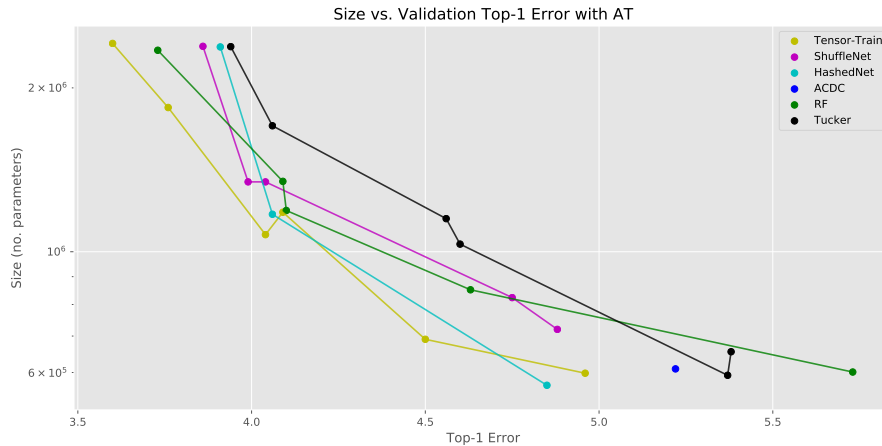


Figure 1: The relationship between top-1 error on the validation set and the number of parameters is plotted for experiments involving WRN-28-10 on CIFAR-10, for experiments using AT. Each substitute linear transform tested is indicated in the legend. On this problem, both Tensor-Train and HashedNet substitutions are able to achieve the highest rates of compression while maintaining performance. At lower compression settings, all methods compared achieve comparable top-1 error.

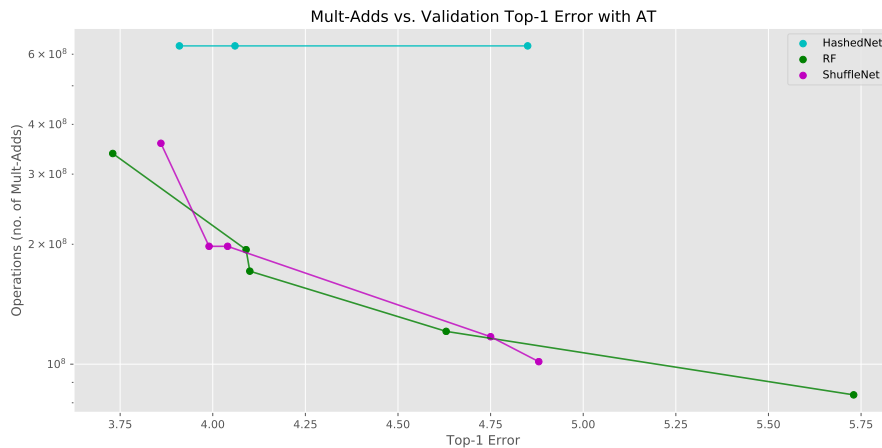


Figure 2: The relationship between top-1 error on the validation set and the number of multi-adds consumed by each network is plotted for experiments involving WRN-28-10 on CIFAR-10. We were unable to calculate robust estimates for the multi-adds used by TT or Tucker substitutions, as they would depend on the choice of rounding and efficient matrix-vector multiplication algorithms used (Oseledets, 2011). The only stable ACDC experiment cost 1.8×10^9 multi-adds, far more than competing methods. Upon investigation, this experiment used a substitution of 12 ACDC layers (as used in the original paper) and this only uses fewer multi-adds than the original linear transform for layers of more than 625 units.

We can see that our networks conveniently explores an *empty region of the Pareto frontier* in the context set by the literature. The top-1 error achieved through a HashedNet substitution is equal to or lower than all published networks compared against, save for DARTS and NASNet-A, while using several times fewer parameters.

When we compute the multi-adds used by these networks (Figure 4) we observe similar trends. Notably, our ShuffleNet substitution performs extremely similarly to the original network while using

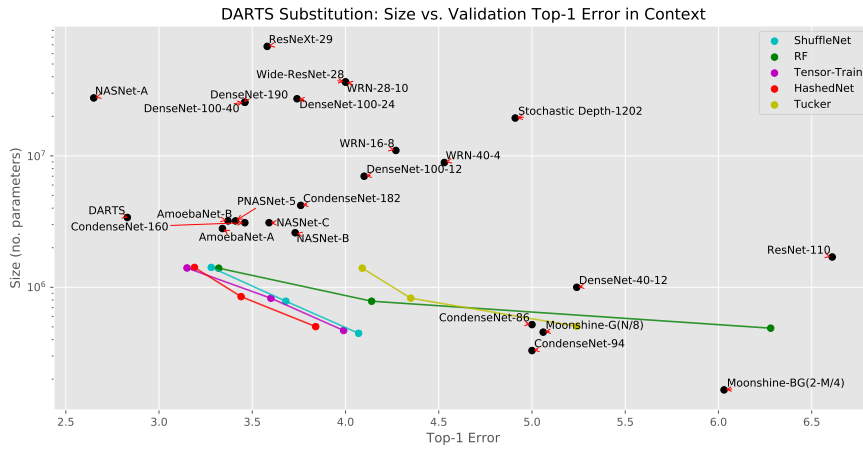


Figure 3: Top-1 validation errors on CIFAR-10 for DARTS networks with substitute linear transforms and their parameter totals. Each substitute linear transform tested is indicated in the legend. ACDC is omitted as it failed to converge below 8% in any case. We compare against recent networks presented in the literature, including: DenseNet (Huang et al., 2017), Moonshine (Crowley et al., 2018), Wide ResNet (Zagoruyko & Komodakis, 2016), ResNeXt (Xie et al., 2017), Stochastic Depth (Huang et al., 2016), GoogleNet (Szegedy et al., 2015), CondenseNet (Huang et al., 2018), NASNet (Zoph et al., 2018), ResNet (He et al., 2016), PNASNet (Liu et al., 2018), AmoebaNet (Real et al., 2018) and DARTS (Liu et al., 2019). *Using these substitutions we are able to explore a new region in the Pareto Frontier.*

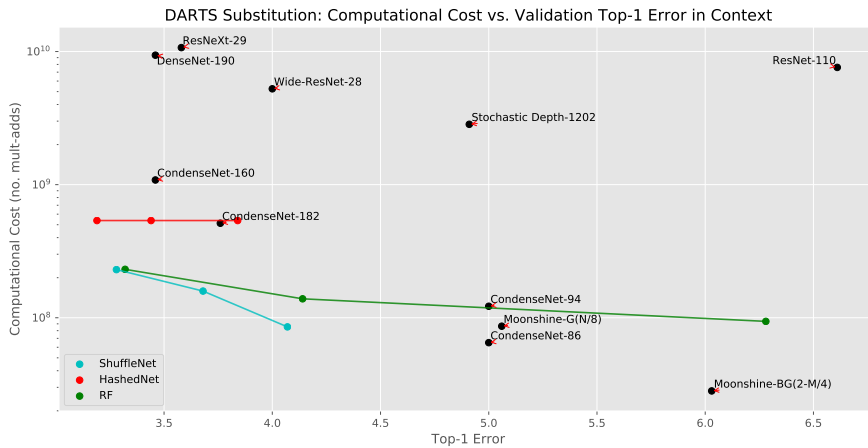


Figure 4: Top-1 validation errors on CIFAR-10 for DARTS networks with substitute linear transforms and their associated multi-add cost. Not all substitute transforms tested could be included here, as noted in Figure 2, not all could be easily estimated. We compare against recent networks in the literature, including: ResNext (Xie et al., 2017), DenseNet (Huang et al., 2017), Wide ResNet (Zagoruyko & Komodakis, 2016), CondenseNet (Huang et al., 2018), Stochastic Depth (Huang et al., 2016), ResNet (He et al., 2016) and Moonshine (Crowley et al., 2018). *On this Figure, ShuffleNet substitutions appear to be Pareto optimal, but we were not able to compare against a large number of papers that do not report multi-add cost on CIFAR-10.*

around 5 times fewer operations. In terms of multi-adds, these networks again extend the Pareto boundary defined by all methods considered.

4.3 WRN-50-2 on ImageNet

Based on their performance in the two CIFAR-10 experiments, we chose HashedNet, Tensor-Train and ShuffleNet to compare on ImageNet with WRN-50-2 as a base network. We also included RF substitution as a baseline.

The results of the experiments are shown in Table 1. ImageNet is a more difficult problem than CIFAR-10, and we see that performance rapidly degrades as we reduce the number of parameters, although this appears to be the same trend observed with published networks in the literature. The compression rates achieved with our agnostic substitutions compare favourably to other state-of-the-art image classification networks in the field. This demonstrates the generalisation of this method to even the largest deep convolutional neural networks for image classification.

Table 1: Top-1 validation errors on ImageNet for WRN-50-2 with our proposed substitutions: ShuffleNet, Tensor-Train and RF. Each method is tested at two approximate parameter budgets. Compression is given as a percentage of the original model size. Methods from the literature are provided for comparison: WRN-50-2 (Zagoruyko & Komodakis, 2016), ShuffleNet (Zhang et al., 2018), DenseNet (Huang et al., 2017), MobileNet (Howard et al., 2017), DecomposeMe (Alvarez & Salzmann, 2017), ACDC (Moczulski et al., 2016) and TT (Novikov et al., 2015).

Model	Substitution	Parameters	Mult-Adds	Top-1 (%)	Compression (%)	
					Parameters	Mult-Adds
WRN-50-2	ShuffleNet	6.04M	0.91G	29.7	8.77	8.00
WRN-50-2	ShuffleNet	17.72M	3.22G	26.9	25.72	28.22
WRN-50-2	RF	4.35M	0.53G	39.8	6.3	4.62
WRN-50-2	RF	17.55M	2.83G	25.4	25.5	24.77
WRN-50-2	HashedNet	4.35M	4.86G	33.5	6.32	42.59
WRN-50-2	HashedNet	17.61M	4.86G	24.5	25.56	42.59
WRN-50-2	Tensor-Train	4.34M	4.86G	33.2	6.30	42.59
WRN-50-2	Tensor-Train	17.58M	4.86G	24.9	25.52	42.59
WRN-50-2		68.9M	11G	21.9		
ShuffleNet		1.87M	0.14G	32.4		
ShuffleNet 2x		7.51M	0.53G	24.7		
DenseNet-121		9M	6G	25.0		
MobileNet		4.2M	0.57G	29.4		
Dec ₈ ⁵¹²			0.45G	33.2	46.5	53.8
CaffeNet(ACDC)		9.7M		43.3	16.7	
VGG-16(TT)		18.65M		32.2	13.5	
VGG-19(TT)		24.0M		31.6	16.7	

5 Ablation Studies

5.1 Training With Distillation

Distillation via attention transfer (Zagoruyko & Komodakis, 2017)—or AT—is used for most of our experiments because we saw it universally improved top-1 validation error in the experiments with WRN-28-10 on CIFAR-10. Figure 5 illustrates the difference in top-1 error validation error in the WRN-28-10 experiments. Almost all methods benefit by more than 1%, which can be critical for a competitive top-1 error score on CIFAR-10. The ACDC substitution was omitted, as it was not stable with AT (but was also not competitive regardless).

Unlike methods, such as a hyperparameter search, that allow us to spend more computation time to achieve a better top-1 error, AT does not require tuning. We did not tune any hyperparameters in any of the experiments presented here. For this reason, we can view AT as a way to compensate for an inadequate training routine.

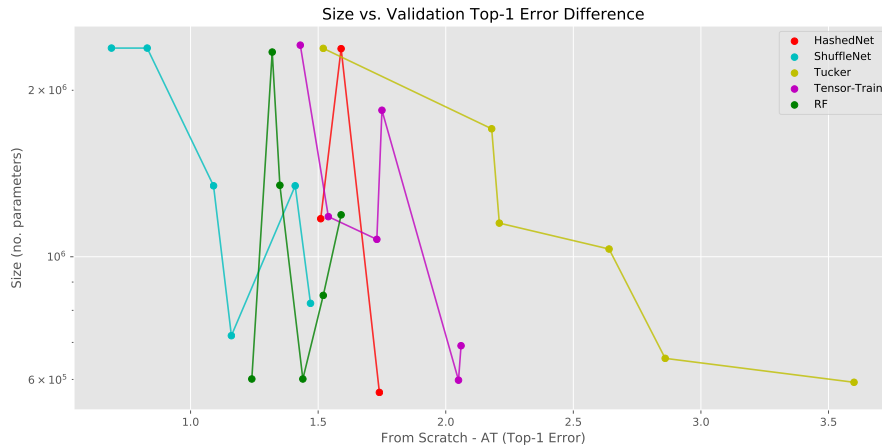


Figure 5: The difference in top-1 validation error with and without AT distillation is plotted for each substitute linear transform applied to WRN-28-10 on the CIFAR-10 classification problem. Over all the linear transform substitutions, AT lowers the top-1 validation error by a few percent. It has the greatest benefit in conjunction with the Tucker substitution, which has a higher overall top-1 validation error, as can be seen in Figure 1.

5.2 CRS Weight Decay Ablation

To justify CRS weight decay, we ran an ablation experiment, repeating the experiments on CIFAR-10 with WRN-28-10, but disabling CRS weight decay. In Figure 6 these results are illustrated. For almost all methods we see that there is a clear benefit. ShuffleNet simply fails to converge without it. However, for HashedNet we see that it is slightly detrimental.

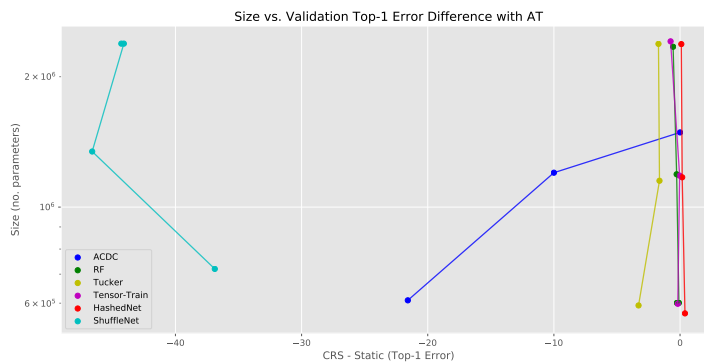


Figure 6: The difference in top-1 error on the validation set of CIFAR-10, when training with and without CRS weight decay, over all the substitution methods considered for WRN-28-10. For all methods apart from HashedNet, this form of weight decay scaling is beneficial; it results in a lower top-1 validation error.

To investigate why this happens, Figure 7 illustrates the learning curves—top-1 error plots against current training epoch—of these HashedNet substitute networks. The CRS weight decay stabilises training as we would hope, and the top-1 validation error is lower with it enabled *until the final stage* of the learning rate schedule. At this stage we can see the training top-1 error decreases faster when CRS weight decay is enabled. This overfitting is enough to cause a slight increase in top-1 error.

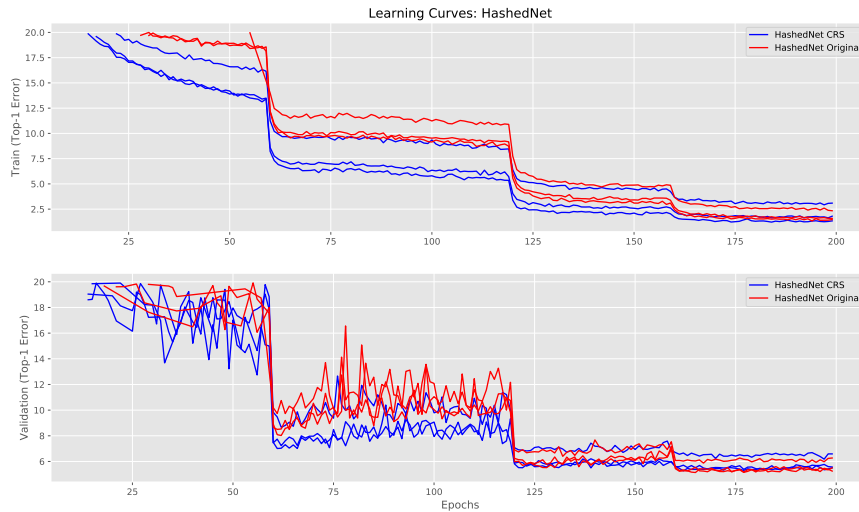


Figure 7: Learning curves for HashedNet substitution experiments, with and without CRS weight decay. When CRS weight decay is enabled the top-1 error is lower, on train and test, at every epoch until the final part of the learning rate schedule.

6 Conclusion

Many alternative efficient dense layers have been proposed in prior work. In this paper we have reviewed a selection of these layers to be substituted into state-of-the-art image classification networks. This was motivated by the potential efficiency benefits, at training and test time, of using such layers in real applications. Training using such layers as substitutes in existing image classification architectures can be trivially stabilised by using CRS weight decay; a rote method to scale the weight decay prescribed for the original architecture. As this does not require hand tuning, it allows many alternatives to expensive convolutional layers to be used. We found that these substitutions were capable of performing efficiently on contemporary image classification benchmarks. We have explored a new region of the Pareto frontier for both parameter and computational cost on CIFAR-10. On ImageNet, we find it is possible to match the compression performance of many published methods, all while using a network in which the weights are a linear reparameterisation of the original.

Acknowledgements This study was supported in part by an EPSRC scholarship granted to GG from the Neuroinformatics and Computational Neuroscience Doctoral Training Centre at the University of Edinburgh, a Huawei DDMPLab Innovation Research Grant, as well as funding from the European Union’s Horizon 2020 research and innovation programme under grant agreement No. 732204 (Bonseyes). This work is supported by the Swiss State Secretariat for Education, Research and Innovation (SERI) under contract number 16.0159. The opinions expressed and arguments employed herein do not necessarily reflect the official views of these funding bodies. The authors are grateful to Rafael Ballester for correspondence on tensor-train practicalities, and to Joseph Mellor for productive discussions on the CRS weight decay scheme and HashedNet.

References

- Alvarez, J. M. and Salzmann, M. Learning the number of neurons in deep networks. In *Advances in Neural Information Processing Systems*, 2016.
- Alvarez, J. M. and Salzmann, M. Compression-aware training of deep networks. In *Advances in Neural Information Processing Systems*, 2017.

- Araujo, A., Negrevergne, B., Chevaleyre, Y., and Atif, J. On the expressive power of deep fully circulant neural networks. *arXiv preprint arXiv:1901.10255*, 2019.
- Ballester, R. tntorch: Tensor network learning with PyTorch. <https://github.com/rballester/tntorch>, 2019. Accessed: 14th February 2019.
- Bojarski, M., Choromanska, A., Choromanski, K., Fagan, F., Gouy-Pailler, C., Morvan, A., Sakr, N., Sarlos, T., and Atif, J. Structured adaptive and random spinners for fast machine learning computations. *arXiv preprint arXiv:1610.06209*, 2016.
- Chen, W., Wilson, J., Tyree, S., Weinberger, K., and Chen, Y. Compressing neural networks with the hashing trick. In *International Conference on Machine Learning*, 2015.
- Cheng, Y., Yu, F. X., Feris, R. S., Kumar, S., Choudhary, A., and Chang, S.-F. An exploration of parameter redundancy in deep networks with circulant projections. In *Proceedings of the IEEE International Conference on Computer Vision*, 2015.
- Courbariaux, M., Bengio, Y., and David, J.-P. BinaryConnect: Training deep neural networks with binary weights during propagations. In *Advances in Neural Information Processing Systems*, 2015.
- Crowley, E. J., Gray, G., and Storkey, A. Moonshine: Distilling with cheap convolutions. In *Advances in Neural Information Processing Systems*, 2018.
- De Sa, C., Gu, A., Puttagunta, R., Ré, C., and Rudra, A. A two-pronged progress in structured dense matrix vector multiplication. In *Proceedings of the ACM-SIAM Symposium on Discrete Algorithms*, 2018.
- DeVries, T. and Taylor, G. W. Improved regularization of convolutional neural networks with cutout. *arXiv preprint arXiv:1708.04552*, 2017.
- Flyamer, I., Colin, Xue, Z., Li, A., Vazquez, V., Morshed, N., Neste, C. V., scaine1, and mski_iksm.adjustText. <https://github.com/Phlya/adjustText>, November 2018.
- Gao, H., Wang, Z., and Ji, S. ChannelNets: Compact and efficient convolutional neural networks via channel-wise convolutions. In *Advances in Neural Information Processing Systems*, 2018.
- Gilbert, E. Theory of shuffling. Technical report, Bell Labs, Murray Hill, New Jersey, U.S., 1955.
- He, K., Zhang, X., Ren, S., and Sun, J. Deep residual learning for image recognition. In *Proceedings of the IEEE Conference on Computer Vision and Pattern Recognition*, 2016.
- Howard, A. G., Zhu, M., Chen, B., Kalenichenko, D., Wang, W., Weyand, T., Andreetto, M., and Adam, H. MobileNets: Efficient convolutional neural networks for mobile vision applications. *arXiv preprint arXiv:1704.04861*, 2017.
- Hu, Z. Torch-DCT. <https://github.com/zh217/torch-dct>, 2019. Accessed: 14th February 2019.
- Huang, G., Sun, Y., Liu, Z., Sedra, D., and Weinberger, K. Q. Deep networks with stochastic depth. In *European Conference on Computer Vision*, 2016.
- Huang, G., Liu, Z., van der Maaten, L., and Weinberger, K. Q. Densely connected convolutional networks. In *Proceedings of the IEEE Conference on Computer Vision and Pattern Recognition*, 2017.
- Huang, G., Liu, S., van der Maaten, L., and Weinberger, K. Q. CondenseNet: An efficient densenet using learned group convolutions. In *Proceedings of the IEEE Conference on Computer Vision and Pattern Recognition*, 2018.
- Hunter, J. D. Matplotlib: A 2D graphics environment. *Computing In Science & Engineering*, 9(3): 90–95, 2007. doi: 10.1109/MCSE.2007.55.
- Jaderberg, M., Vedaldi, A., and Zisserman, A. Speeding up convolutional neural networks with low rank expansions. In *British Machine Vision Conference*, 2014.

- Kim, Y.-D., Park, E., Yoo, S., Choi, T., Yang, L., and Shin, D. Compression of deep convolutional neural networks for fast and low power mobile applications. *ArXiv e-prints*, November 2015.
- Kossaiji, J., Lipton, Z., Khanna, A., Furlanello, T., and Anandkumar, A. Tensor regression networks. *arXiv preprint arXiv:1708.04552*, 2017.
- Krizhevsky, A. Learning multiple layers of features from tiny images. Master’s thesis, University of Toronto, 2009.
- LeCun, Y., Denker, J. S., and Solla, S. A. Optimal brain damage. In *Advances in Neural Information Processing Systems*, 1989.
- Liao, S., Li, Z., Zhao, L., Qiu, Q., Wang, Y., and Yuan, B. CircConv: A structured convolution with low complexity. *arXiv preprint arXiv:1902.11268*, 2019.
- Liu, C., Zoph, B., Neumann, M., Shlens, J., Hua, W., Li, L.-J., Fei-Fei, L., Yuille, A., Huang, J., and Murphy, K. Progressive neural architecture search. In *European Conference on Computer Vision*, 2018.
- Liu, H., Simonyan, K., and Yang, Y. DARTS: Differentiable architecture search. In *International Conference on Learning Representations*, 2019.
- Lu, Z., Sindhvani, V., and Sainath, T. N. Learning compact recurrent neural networks. In *Proceedings of the IEEE International Conference on Acoustics, Speech and Signal Processing*, 2016.
- Moczulski, M., Denil, M., Appleyard, J., and de Freitas, N. ACDC: a structured efficient linear layer. In *International Conference on Learning Representations*, 2016.
- Murphy, K. P. *Machine Learning: A Probabilistic Perspective*. The MIT Press, London, 2012. ISBN 978-0-262-01802-0. URL <http://dl.acm.org/citation.cfm?id=2380985>.
- Novikov, A., Podoprikin, D., Osokin, A., and Vetrov, D. P. Tensorizing neural networks. In *Advances in Neural Information Processing Systems*, 2015.
- Oseledets, I. V. Tensor-train decomposition. *SIAM Journal on Scientific Computing*, 33(5):2295–2317, 2011.
- Paszke, A., Gross, S., Chintala, S., and Chanan, G. PyTorch: Tensors and dynamic neural networks in Python with strong GPU acceleration. <https://github.com/pytorch/pytorch>, 2019. Accessed: 14th February 2019.
- Real, E., Aggarwal, A., Huang, Y., and Le, Q. V. Regularized evolution for image classifier architecture search. *arXiv preprint arXiv:1802.01548*, 2018.
- Russakovsky, O., Deng, J., Su, H., Krause, J., Satheesh, S., Ma, S., Huang, Z., Karpathy, A., Khosla, A., Bernstein, M., Berg, A. C., and Fei-Fei, L. ImageNet large scale visual recognition challenge. *Int. Journal of Computer Vision (IJCV)*, 115(3):211–252, 2015. doi: 10.1007/s11263-015-0816-y.
- Sainath, T. N., Kingsbury, B., Sindhvani, V., Arisoy, E., and Ramabhadran, B. Low-rank matrix factorization for deep neural network training with high-dimensional output targets. In *Proceedings of the IEEE International Conference on Acoustics, Speech and Signal Processing*, 2013.
- Sindhvani, V., Sainath, T. N., and Kumar, S. Structured transforms for small-footprint deep learning. In *Advances in Neural Information Processing Systems*, 2015.
- Stevens, J.-L. R., Rudiger, P., and Bednar, J. A. Holoviews: Building complex visualizations easily for reproducible science. In *SciPy Conference Proceedings*, 2015. doi: 10.25080/Majora-7b98e3ed-00a. URL <http://holoviews.org/>.
- Szegedy, C., Liu, W., Jia, Y., Sermanet, P., Reed, S., Anguelov, D., Erhan, D., Vanhoucke, V., and Rabinovich, A. Going deeper with convolutions. In *Proceedings of the IEEE Conference on Computer Vision and Pattern Recognition*, 2015.
- Thomas, A., Gu, A., Dao, T., Rudra, A., and Ré, C. Learning compressed transforms with low displacement rank. In *Advances in Neural Information Processing Systems*, 2018.

- Xie, S., Girshick, R., Dollár, P., Tu, Z., and He, K. Aggregated residual transformations for deep neural networks. In *Proceedings of the IEEE Conference on Computer Vision and Pattern Recognition*, 2017.
- Yang, Z., Moczulski, M., Denil, M., de Freitas, N., Smola, A., Song, L., and Wang, Z. Deep fried convnets. In *Proceedings of the IEEE Conference on Computer Vision and Pattern Recognition*, 2015.
- Zagoruyko, S. and Komodakis, N. Wide residual networks. In *British Machine Vision Conference*, 2016.
- Zagoruyko, S. and Komodakis, N. Paying more attention to attention: Improving the performance of convolutional neural networks via attention transfer. In *International Conference on Learning Representations*, 2017.
- Zhang, X., Zhou, X., Lin, M., and Sun, J. ShuffleNet: An extremely efficient convolutional neural network for mobile devices. In *Proceedings of the IEEE Conference on Computer Vision and Pattern Recognition*, 2018.
- Zhao, L., Liao, S., Wang, Y., Li, Z., Tang, J., and Yuan, B. Theoretical properties for neural networks with weight matrices of low displacement rank. In *International Conference on Machine Learning*, 2017.
- Zhao, R., Hu, Y., Dotzel, J., Sa, C. D., and Zhang, Z. Building efficient deep neural networks with unitary group convolutions. In *Proceedings of the IEEE Conference on Computer Vision and Pattern Recognition*, 2019.
- Zoph, B. and Le, Q. V. Neural architecture search with reinforcement learning. In *International Conference on Learning Representations*, 2017.
- Zoph, B., Vasudevan, V., Shlens, J., and Le, Q. V. Learning transferable architectures for scalable image recognition. In *Proceedings of the IEEE Conference on Computer Vision and Pattern Recognition*, 2018.

A HashedNet Disconnected Weights

The indices produced by the hash function are approximately uniform over the set of real weights. This produces a weight matrix in which weights are randomly tied, with each unique weight occurring on average the same number of times. Chen et al. (2015) demonstrate that the cost of accessing these weights is negligible at test time. In our experiments, we do not use a hash function, instead sampling the indices once when the layer is initialised and storing them.

The number of parameters to be optimised here is the number of *real* weights \mathbf{w} , which can be set to be 1 or greater, up to the number of elements in the virtual weight matrix. However, as the number of real weights is increased the probability we may store a weight that is never used in the virtual weight matrix increases. If N_r is the number of real weights and N_v is the number of virtual weights, then the expected number of weights that will be excluded will be $N_r(1 - 1/N_r)^{N_v}$. Defining N_r in terms of N_v using a compression ratio $c = \frac{N_r}{N_v}$, we can investigate what happens to the ratio excluded, e , as c changes:

$$e = \left(1 - \frac{1}{cN_v}\right)^{N_v} \tag{9}$$

$$= \exp\left(N_v \log\left(1 - \frac{1}{cN_v}\right)\right). \tag{10}$$

Taking the Taylor expansion of $\log\left(1 - \frac{1}{cN_v}\right)$ and retaining the first two terms:

$$e = \exp\left(N_v \log\left(1 - \frac{1}{cN_v}\right)\right) \tag{11}$$

$$= \exp\left(N_v \left(-\frac{1}{cN_v} + O\left(\frac{1}{(cN_v)^2}\right)\right)\right) \tag{12}$$

$$\approx \lim_{N_v \rightarrow \infty} \exp\left(N_v \left(-\frac{1}{cN_v} + O\left(\frac{1}{(cN_v)^2}\right)\right)\right) \tag{13}$$

$$= \exp\left(-\frac{N_v}{cN_v}\right) \tag{14}$$

$$= \exp\left(-\frac{1}{c}\right). \tag{15}$$

As shown in Figure 8, this limit argument holds true for the values of N_v we are interested in, and the proportion of weights excluded as the compression ratio grows can be significant. In our experiments we do not address these wasted parameters, despite performing experiments with compression ratios in regions where 10-20% of our parameters are being excluded. It would also be possible to identify these parameters and choose not to store them, but we do not investigate this. The reason being that we find the HashedNet substitution effective at high compression levels, such as below $c = 0.1$, and in this region a negligible number of weights will be excluded.

B Chosen Parameter Budgets

After normalising the tuning of all layers between 0 and 1, we can plot number of parameters used by each substitution as shown in Figure 9. The upper limit and lower limits were chosen where all methods have support. For example, we can see in Figure 9 we can see that the upper limit is defined by the Linear ShuffleNet, while the lower limit is defined by RF. We chose the midpoint by linear interpolation in log parameter count.

C Experiment Setup

All experiments were written in Python using PyTorch (Paszke et al., 2019). Tensor-Train and Tucker decompositions were implemented using tntorch (Ballester, 2019); all other methods were implemented separately. The code implementing ACDC layers is based on the work of Hu (2019),

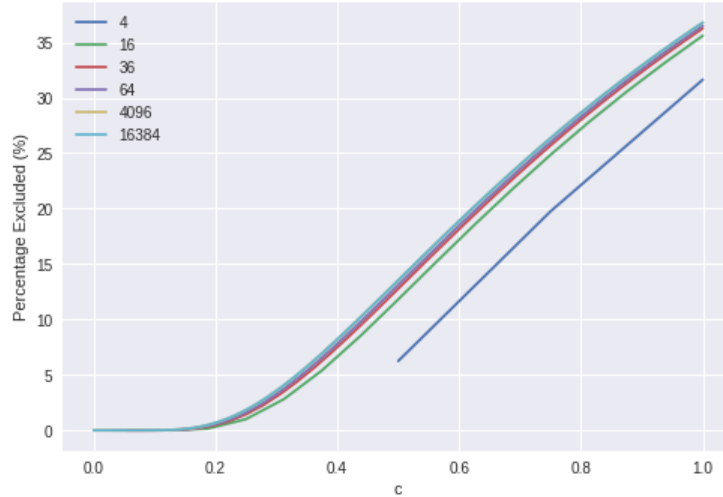


Figure 8: The effect on percentage of weights excluded depending on compression ratio c , tested for different values of N_v , the number of elements in the virtual weight matrix, indicated in the legend. At the compression levels we are interested in—20% of the original number of weights—we can see that the number of weights excluded is low.

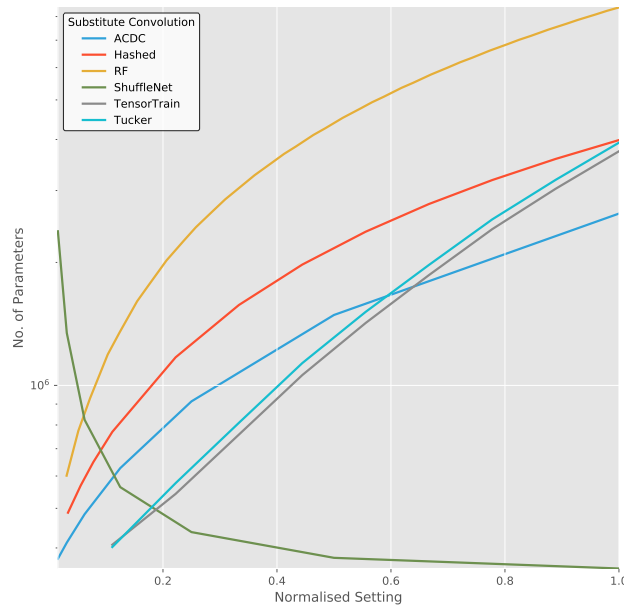


Figure 9: The parameter cost of a WRN-28-10 after substitution by the methods listed in the legend, varying the tunable parameter of each over a normalised range. We design experiments over a parameter count range such that all methods illustrated will have support, which here is limited by the maximum size of the Linear ShuffleNet and the minimum size of the RF substitution.

and is publicly available: <https://github.com/gngdb/pytorch-acdc>. Figures were produced using Matplotlib (Hunter, 2007) and Holoviews (Stevens et al., 2015). Annotations on figures were placed using adjustText (Flyamer et al., 2018).

CIFAR-10 is a set of 60,000 colour images of size 32 by 32 pixels, with the task of classifying each image according to 10 classes (Krizhevsky, 2009). ImageNet is a dataset of over a million colour images of size 224 by 224, with the task of classifying each into 1000 classes (Russakovsky et al.,

2015). The results on CIFAR-10 typically inform experiments planned on ImageNet, which is used as verification that the method scales to large problems.

For CIFAR-10 experiments we focused on two architectures: Wide ResNets (Zagoruyko & Komodakis, 2016) (WRN) and the network found in Liu et al. (2019) (DARTS). Wide ResNets were chosen to demonstrate results on a common ResNet structure. Results on this type of network should be reflected in many similar networks in the literature. Wide ResNets are defined by their *depth* and *width* factors. We choose to focus on the WRN-28-10, depth = 28 and width = 10 in Zagoruyko & Komodakis (2016).

Wide ResNet architectures were used to demonstrate the results of attention transfer (Zagoruyko & Komodakis, 2017), and we run these networks using that training protocol. When using attention transfer β was set to 1000.

DARTS was selected in order to demonstrate results on a state-of-the-art image classification architecture. We replicated precisely the training hyperparameters and schedule used in the original paper.

Wide ResNet Each network was trained for 200 epochs with a learning rate starting at 0.1 and scaled by 0.2 on epochs 60, 120 and 160. Momentum was set to 0.9 and the minibatch size was 128. Weight decay was set to 5×10^{-4} and scaled in all experiments according to the method described in Section 3.2, apart from the ablation experiment described in Section 5.2. Data was augmented with random crops, left-right flips and Cutout (DeVries & Taylor, 2017).

DARTS Each network was trained for 600 epochs using a cosine annealed learning rate schedule starting at 0.025. Momentum was set to 0.9 and the minibatch size was 96. Weight decay was set to 3×10^{-4} and scaled in all experiments according to the method described in Section 3.2. The auxiliary classification head was used in training, but not counted at test time, and the drop-path method from the paper followed the same schedule of a linear increase in drop probability from 0 to 0.2 over the learning schedule. Data was again augmented with random crops, left-right flips and Cutout (DeVries & Taylor, 2017).

In ImageNet experiments we focused on a large network with competitive results, in order to demonstrate the potential for compression. As with previous experiments we chose a Wide ResNet (Zagoruyko & Komodakis, 2016), so that results could be interpreted as transferable to other ResNet-like architectures in the literature. All ImageNet experiments use the WRN-50-2, which is precisely a ResNet-50 (He et al., 2016) with twice as many channels on inner bottlenecks. The published performance of 21.9% top-1 error is competitive with the best published results on ImageNet. We used the publicly available model zoo trained weights and found it could only achieve 22.5%, but chose to use this network regardless.

Each network was trained for 90 epochs with a learning rate of 0.1 scaled by 0.1 at epochs 30 and 60. Momentum was set to 0.9 and the minibatch size was 256. Weight decay was 1×10^{-4} and scaled according to the method described in Section 3.2. Data was augmented with random crops and left-right flips.